RSC Advances

COMMUNICATION

Mercaptophenylboronic acid modified gold nanoparticle@silica bubbles for buoyant separation and specific enrichment of glycopeptides†

Cite this: *RSC Adv.*, 2014, **4**, 28856

Received 25th April 2014
Accepted 23rd June 2014

DOI: 10.1039/c4ra03769c

www.rsc.org/advances

Junjie Hu, Rongna Ma, Fei Liu, Yunlong Chen and Huangxian Ju*

A buoyant separation method was proposed by using mercaptophenylboronic acid modified gold nanoparticles @silica bubbles, a new functional low-density material, for specific enrichment of glycopeptides.

As one of the most significant post-translational modifications, glycosylation is involved in a number of biological processes, including protein folding, signal transduction, immune response and cell recognition.[1] Therefore, the separation and enrichment of glycopeptides or glycoproteins are extremely important. So far many strategies have been raised to achieve glycol-specific enrichment, such as lectin-based affinity chromatography,[2] hydrophilic interaction liquid chromatography,[3] size exclusion chromatography[4] and hydrazide chemistry.[5] Besides, boronic acid-based enrichment methods have also attracted considerable attention due to the specific recognition of boronic acid to the *cis*-diol OH-containing structures existing in most sugar moieties.[6] Boronic acid functionalized mesoporous silica,[6a] agarose resin[6b] and monoliths[6d,e] have been used to enrich glycopeptides. However, the enrichment procedures usually require high-speed centrifugation, which leads to both time consuming and the loss of low-abundance glycopeptides. Although some magnetic materials can be used to easily separate the captured protein, an external magnet is necessary.[7] Thus there is a high demand to probe the new materials for separation of targets from complex biological samples.

Recently, hollow silica bubbles (SiBs) have been used for surface-enhanced Raman scattering analysis.[8] This material can float over the solution. In view of the advantages of gold nanoparticles (AuNPs) in biological analysis,[9] this work used AuNPs to functionalize silica bubbles (Au@SiBs) and synthesized mercaptophenylboronic acid (MPB) modified Au@SiBs. The newly designed material led to a buoyant separation method for specific enrichment of glycopeptides (Scheme 1).

The synthesis of MPB-Au@SiBs was illustrated in Scheme 1A, which mainly included three steps, *i.e.* silanizing the SiBs with 3-aminopropyltriethoxysilane (APTES) overnight, controllable assembly of AuNPs on bubble surface *via* the interaction between amino group and AuNPs, and functionalizing Au@SiBs with MPB *via* Au–S bond (ESI). Benefited from the unique buoyant separability of MPB-Au@SiBs and large amount of boronic groups on the bubble surface, the MPB-Au@SiBs could efficiently capture glycopeptides, rapidly separate the targets from biological samples and conveniently release the captured targets for following mass spectroscopic (MS) analysis by

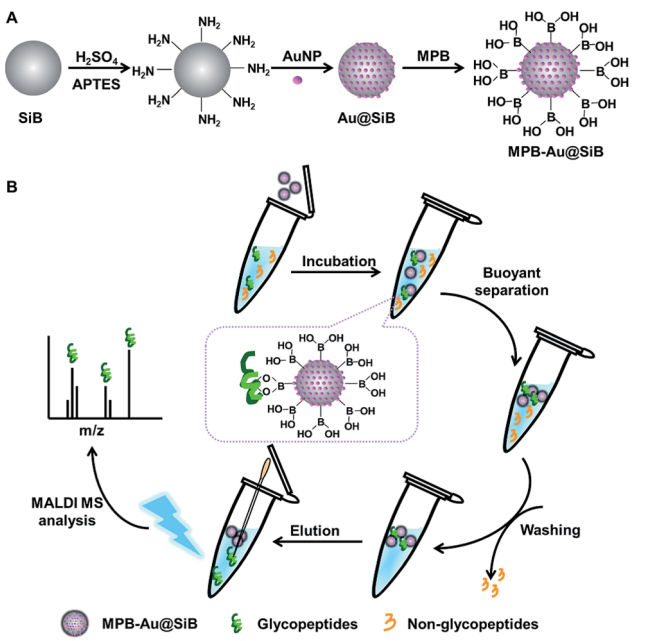

Scheme 1 (A) Synthesis of MPB-Au@SiBs, (B) buoyant separation and specific enrichment of glycopeptides from biological samples for MS analysis.

State Key Laboratory of Analytical Chemistry for Life Science, School of Chemistry and Chemical Engineering, Nanjing University, Nanjing 210093, P.R. China. E-mail: hxju@nju.edu.cn; Fax: +86 25 83593593; Tel: +86 25 83593593

† Electronic supplementary information (ESI) available: Experimental details and additional figures. See DOI: 10.1039/c4ra03769c

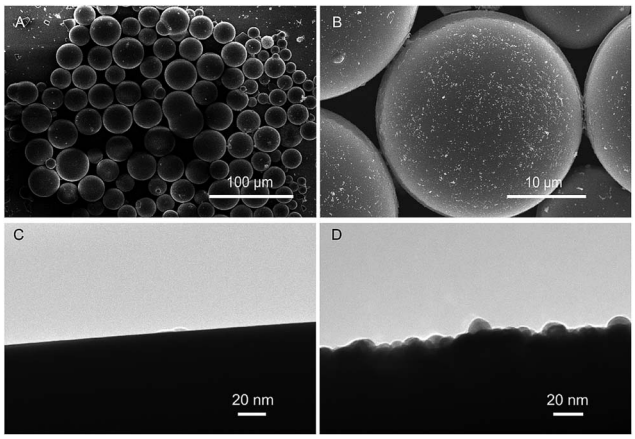

Fig. 1 SEM images of MPB-Au@SiBs under (A) low and (B) high magnifications. TEM images of (C) SiBs and (D) Au@SiBs.

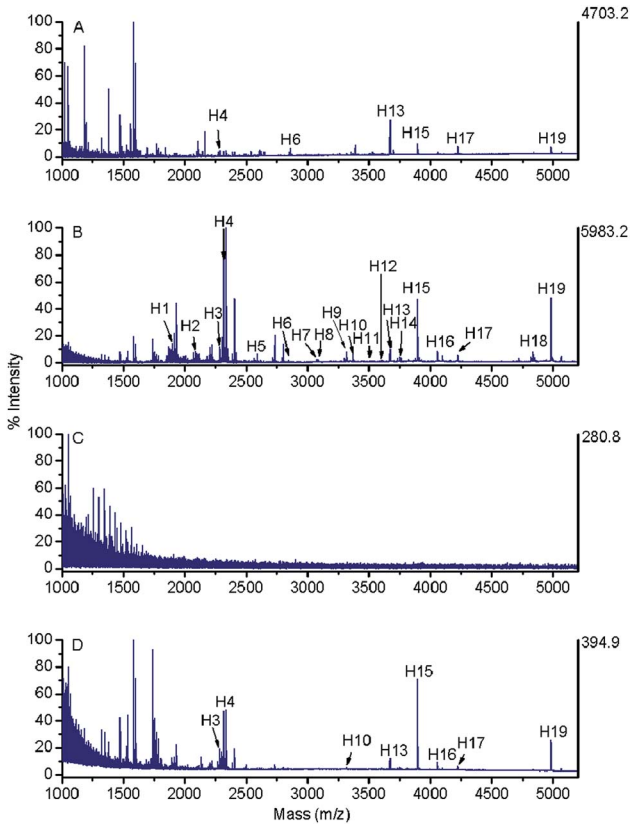

Fig. 2 MALDI-TOF MS spectra of 5 ng μL^{-1} HRP tryptic digest (A) without and with (B) enrichment with MPB-Au@SiBs, (C) Au@SiBs and (D) commercial APB agarose. Glycopeptides above were marked.

reversible covalent binding of the boronic group with the hydroxyl groups of glycopeptides (Scheme 1B).

Owing to the low density of SiBs (0.6 g cm^{-3}), both Au@SiBs and MPB-Au@SiBs could easily float to the upper layer of solution (Fig. S1A in ESI†). After loading of AuNPs onto the silanized SiBs surface, the colour of the material turned from white (a) to purple (b). The binding of MPB to AuNPs also led to obvious change of the colour (c). The FT-IR spectra of these modified SiBs showed a broad absorption band around 3448 cm^{-1}, which was assigned to the stretching vibration of surface hydroxyl group, a N–H stretching vibration band at 1637 cm^{-1} and a Si–O–Si stretching vibration at 1077 cm^{-1} (Fig. S1B in ESI†). The presence of N–H stretching vibration confirmed the successful silanization of the silica bubbles by APTES. After assembly of AuNPs and followed binding of MPB, the FT-IR spectrum showed an obvious B–O adsorption at 1398 cm^{-1} and a *p*-benzene ring distorting vibration at 797 cm^{-1} (curve c), indicating the presence of MPB on the functional surface.

The scanning electron microscopic (SEM) image of the as-prepared MPB-Au@SiBs revealed the good dispersity with an average diameter of 30 μm (Fig. 1A). Under high magnification the SEM image displayed bright "AuNPs islands" with a uniform distribution (Fig. 1B), indicating the successful AuNPs assembly on the microsphere surface. Further magnification of TEM images confirmed the presence of compact AuNPs (Fig. 1C and D). The synthesis of MPB-Au@SiBs was further confirmed by X-ray photoelectron spectroscopic spectra, in which obvious Au4f peaks at 85.9 and 89.5 eV and B1s peak at 192.3 eV were observed (Fig. S2 in ESI†). In addition, the amount of MPB bound on the surface of Au@SiBs was estimated to be 43.5 μg mg^{-1} with liquid chromatographic analysis (ESI).

Contact angles were tested by fixing the materials to the glass slides and spotting 1 μL of water on the substrates to evaluate the hydrophilicity of the materials. The silanization led to the decrease of contact angle from 83.2° to 26.2° due to the introduction of hydroxyl and amino groups to the surface (Fig. S3A and S3B in ESI†). After loading of AuNPs and binding of MPB, the contact angle tuned to 43.0° and 26.1°, respectively (Fig. S3C and 3D in ESI†). The good hydrophilicity of MPB-Au@SiBs would benefit the dispersity in aqueous solution and the enrichment of glycopeptides.

The specific recognition between MPB-Au@SiBs and glycopeptides was based on the borate esterification reaction, in which a heterocyclic diester was formed by the reaction of boronic group with glycopeptides in an alkaline solution. Importantly the esters could be dissociated by switching the solution to acidic pH. Thus the reversible release of the captured glycopeptides could be achieved. In order to indentify this property, tryptic digest of horseradish peroxidase (HRP) were employed for MALDI-TOF MS analysis. As shown in Fig. 2A, the direct detection showed only 6 peaks of glycopeptides (labelled with H4, H6, H13, H15, H17 and H19), moreover, these signal were relatively weak due to the suppressing of non-glycopeptides with higher abundance in the sample. After enrichment with MPB-Au@SiBs, the mass spectrum could showed other 13 glycosylated peptides, while most non-glycopeptides in low *m*/*z* range were efficiently inhibited (Fig. 2B). The amount of detectable peaks was more than those previously reported boronic acid functionalized mesoporous silica (5),[6a] boronic acid modified gold microspot (16)[10a] and boronic acid functionalized core-satellite composite nanoparticles (17).[10b] The signal-to-noise (*S*/*N*) ratios for glycopeptides detection were also enhanced obviously. For example, after enrichment with MPB-Au@SiBs the *S*/*N* ratios for H4, H15 and H19 increased from 15, 21 and 7 to 285, 80 and 68, respectively. Detailed

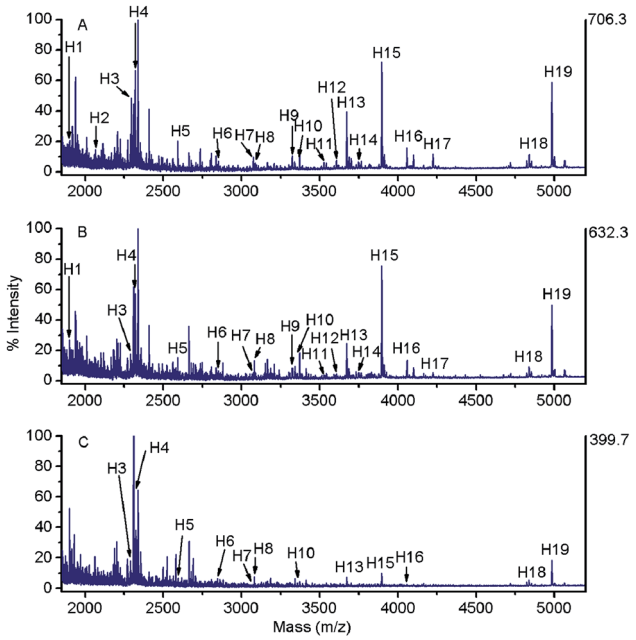

Fig. 3 MALDI mass spectra of trypic digest mixtures of HRP and BSA at (A) 1 : 1, (B) 1 : 10 and (C) 1 : 20 after enrichment with MPB-Au@SiBs.

sequence information of these detectable glycopeptides was listed in Table S1 in ESI.† The binding capacity of glycopeptides to MPB-Au@SiBs was evaluated to be around 60 mg g^{-1} (Fig. S4 in ESI†), which was higher than 24 mg g^{-1} of magnetic silica particles functionalized with boronic acid.[10b]

As control, Au@SiBs and commercial APB agarose were also applied to enrich glycopeptides. After capture with Au@SiBs, almost no glycopeptide was detected by MALDI-TOF MS (Fig. 2C), suggesting that MPB played a key role for glycopeptides enrichment. The mass spectrum of glycopeptides after enrichment with commercial APB agarose showed only 8 peaks (Fig. 2D), much lower than the number detected after the enrichment with MPB-Au@SiBs. Therefore, the excellent performance of MPB-Au@SiBs was attributed to both the presence of MPB and the highly efficient buoyant separation.

Different concentrations of HRP tryptic digests were used to test the sensitivity. Even at a concentration of 0.1 ng μL^{-1}, 10 glycopeptide peaks could be detected after enrichment with MPB-Au@SiBs (Fig. S5 in ESI†). Meanwhile, only 1 glycopeptide peak was observed after enrichment with commercial APB agarose even at 10 times higher concentration (Fig. S6 in ESI†). The detection limit (0.1 ng μL^{-1}) was comparable with our previous report using boronic acid functionalized magnetic carbon nanotubes (0.1 ng μL^{-1})[7a] and better than boronic acid functionalized core–shell polymer nanoparticles (1 ng μL^{-1}).[6c]

Similarly, human IgG tryptic digests were further employed to test the robustness of the material. Direct analysis of human IgG tryptic digests showed only 3 and 2 peaks of glycopeptides at 5 and 0.5 ng μL^{-1}, respectively (Fig. S7A and 7B in ESI†). After enrichment with MPB-Au@SiBs, 16 peaks of glycopeptides at 5 ng μL^{-1} could be observed (Fig. S7C and Table S2 in ESI†). The enrichment of commercial APB agarose in the same IgG tryptic digest showed 8 peaks with relatively lower intensities and *S*/*N* ratio (Fig. S7E in ESI†). These results demonstrated that the enrichment of MPB-Au@SiBs was suitable for different kinds of glycopeptides, and MPB-Au@SiBs could be used to capture glycopeptides at lower concentration compared to commercial APB agarose (Fig. S7D and F in ESI†).

Finally, the enrichment selectivity of the MPB-Au@SiBs was examined with the tryptic digest mixture of BSA and HRP at different mass ratios (from 1 : 1 to 20 : 1). As shown in Fig. 3, at the same mass concentration, the presence of BSA did not affect the capture of glycopeptides. With the increasing amount of BSA, the peak intensities of glycopeptides gradually decreased probably because large amounts of nonglycosylated peptides inhibited the binding process. However, 12 peaks of glycopeptides could still be observed in the presence of 20 times nonglycopeptides. These results indicated the acceptable enrichment selectivity of the MPB-Au@SiBs. Moreover, SEM image (Fig. S8 in ESI†) of MPB-Au@SiBs after usage did not show obvious fractures, indicating suitable mechanical stability of the bubbles.

In summary, the low density of SiBs led to a novel method for buoyant separation. The successful functionalization of SiBs with AuNPs and MPB endowed SiBs with good recognition property for enrichment of glycopeptides. The reversible release of captured glycopeptides could be achieved by simply changing solution acidity. Both the specific recognition of MPB to glycopeptides and the highly efficient buoyant separation led to the excellent performance of MPB-Au@SiBs for selective enrichment of glycopeptides. The buoyant capacity of the silica bubbles simplified the separation of glycopeptides from biological samples, thus possessed potential application in high-throughput glycoproteome analysis.

This research was financially supported by the National Basic Research Program of China (2010CB732400), and the National Natural Science Foundation of China (21135002, 21121091, 91213301).

Notes and references

1 (*a*) J. Nilsson, U. Rüetschi, A. Halim, C. Hesse, E. Carlsohn, G. Brikmalm and G. Larson, *Nat. Methods*, 2009, **6**, 809; (*b*) L. Wells, K. Vosseller and G. W. Hart, *Science*, 2001, **291**, 2376; (*c*) P. M. Rudd, T. Elliott, P. Cresswell, I. A. Wilson and R. A. Dwek, *Science*, 2001, **291**, 2370.

2 (*a*) H. Kaji, H. Saito, Y. Yamauchi, T. Shinkawa, M. Taoka, J. Hirabayashi, K. Kasai, N. Takahashi and T. Isobe, *Nat. Biotecnol.*, 2003, **21**, 667; (*b*) J. Nawarak, S. Phutrakul and S. T. Chen, *J. Proteome Res.*, 2004, **3**, 383; (*c*) F. M. Okanda and Z. E. Rassi, *Electrophoresis*, 2006, **27**, 1020; (*d*) E. H. Donnelly and I. J. Goldstein, *Biochem. J.*, 1970, **118**, 679; (*e*) Y. T. Pan, H. H. Bai, C. Ma, Y. L. Deng, W. J. Qin and X. H. Qian, *Talanta*, 2013, **115**, 842.

3 (*a*) Y. Wada, M. Tajiri and S. Yoshida, *Anal. Chem.*, 2004, **76**, 6560; (*b*) M. H. J. Selman, M. Hemayatkar, A. M. Deelder and M. Wuhrer, *Anal. Chem.*, 2011, **83**, 2492; (*c*) G. Palmisano,

S. E. Lendal, K. Engholm-Keller, R. Leth-Larsen, B. L. Parker and M. R. Larsen, *Nat. Protoc.*, 2010, **5**, 1974.

4 (*a*) G. A. Manilla, J. Atwood, Y. Guo, N. L. Warren, R. Orlando and M. Pierce, *J. Proteome Res.*, 2006, **5**, 701; (*b*) D. F. Zielinska, F. Gnad, J. R. Wisniewski and M. Mann, *Cell*, 2010, **141**, 897.

5 (*a*) H. Zhang, X. J. Li, D. B. Martin and R. Aebersold, *Nat. Biotechnol.*, 2003, **21**, 660; (*b*) T. Liu, W. J. Qian, M. A. Gritsenko, D. G. Camp II, M. E. Monroe, R. J. Moore and R. D. Smith, *J. Proteome Res.*, 2005, **4**, 2070; (*c*) B. Y. Sun, J. A. Ranish, A. G. Utleg, J. T. White, X. W. Yan, B. Y. Lin and L. Hood, *Mol. Cell. Proteomics*, 2007, **6**, 141.

6 (*a*) Y. W. Xu, Z. X. Wu, L. J. Zhang, H. J. Lu, P. Y. Yang, P. A. Webley and D. Y. Zhao, *Anal. Chem.*, 2009, **81**, 503; (*b*) Q. B. Zhang, A. A. Schepmoes, J. W. C. Brock, S. Wu, R. J. Moore, S. O. Purvine, J. W. Baynes, R. D. Smith and T. O. Metz, *Anal. Chem.*, 2008, **80**, 9822; (*c*) Y. Y. Qu, J. X. Liu, K. G. Yang, Z. Liang, L. H. Zhang and Y. K. Zhang, *Chem.–Eur. J.*, 2012, **18**, 9056; (*d*) X. L. Sun, R. Liu, X. W. He, L. X. Chen and Y. K. Zhang, *Talanta*, 2010, **81**, 856; (*e*) H. Y. Li and Z. Liu, *TrAC, Trends Anal. Chem.*, 2012, **37**, 148.

7 (*a*) R. N. Ma, J. J. Hu, Z. W. Cai and H. X. Ju, *Nanoscale*, 2014, **6**, 3150; (*b*) W. Zhou, N. Yao, G. P. Yao, C. H. Deng, X. M. Zhang and P. Y. Yang, *Chem. Commun.*, 2008, 5577.

8 (*a*) V. L. Schmit, R. Martoglio, B. Scott, A. D. Strickland and K. T. Carron, *J. Am. Chem. Soc.*, 2012, **134**, 59; (*b*) V. L. Schmit, R. Martoglio and K. T. Carron, *Anal. Chem.*, 2012, **84**, 4233.

9 (*a*) J. Tang, Y. C. Liu, G. P. Yao, C. H. Deng and X. M. Zhang, *Proteomics*, 2009, **9**, 5046; (*b*) G. P. Yao, H. Y. Zhang, C. H. Deng, H. J. Lu, X. M. Zhang and P. Y. Yang, *Rapid Commun. Mass Spectrom.*, 2009, **23**, 3493; (*c*) D. W. Qi, H. Y. Zhang, J. Tang, C. H. Deng and X. M. Zhang, *J. Phys. Chem. C*, 2010, **114**, 9221.

10 (*a*) Z. F. Zhou, Y. D. Wang, X. H. Guo, L. Wang and N. Lu, *Analyst*, 2013, **138**, 3032; (*b*) L. J. Zhang, Y. W. Xu, H. L. Yao, L. Q. Xie, J. Yao, H. J. Lu and P. Y. Yang, *Chem.–Eur. J.*, 2009, **15**, 10158.